

## NUMERICAL ANALYSIS OF CARRIER STATISTICS IN LOW-DIMENSIONAL NANOSTRUCTURE DEVICES

ISMAIL SAAD<sup>1\*</sup>, M. TAGHI AHMADI<sup>2</sup>, MUNAWAR A. RIYADI<sup>3</sup>,  
RAZALI ISMAIL<sup>4</sup> & VIJAY K. ARORA<sup>5</sup>

**Abstract.** The carrier statistics for low-dimensional nanostructure is elaborated. The density of state (DOS) is proportional to  $\lambda_d^d$  where  $d$  is the dimensionality of the nanostructure and  $\lambda_d$  is the De-Broglie wavelength proportion of Fermi-Dirac (FD) integral that covers the carrier statistics to all degeneracy level. In the non-degenerate regime the results replicate what is expected from the Boltzmann statistics. However, the results vary in degenerate regime. The results for all dimensions are numerically analyzed and compared for all three Cartesian directions. With appropriate DOS, the carrier concentration in all dimensions is obtained based on the FD statistic. Fermi energy with respect to band edge is a function of temperature that is independent of the carrier concentration in the non-degenerate regime. In the strongly degenerate regime, the Fermi energy is a function of carrier concentration appropriate for given dimensionality, but is independent of temperature.

**Keywords:** Carrier statistics; carrier concentration; one dimensional devices; degenerate and non-degenerate carrier

**Abstrak.** Statistik pembawa bagi dimensi-bawah strukturan adalah diperjelaskan. Ketumpatan kawasan (DOS) adalah bersamaan dengan  $\lambda_d^d$ , di mana  $d$  ialah dimensi bagi strukturan dan  $\lambda_d$  ialah gelombang De-Broglie bersamaan dengan kamiran Fermi-Dirac yang merangkumi statistik pembawa bagi semua tahap kemerosotan. Pada regim tak-merosot, hasil kajian menunjukkan pengreplikan apa yang ditafsirkan dari statistik Boltzman. Akan tetapi, pada regim merosot hasil adalah berubah-ubah. Hasil bagi semua dimensi telah dianalisis secara berangka dan dibandingkan bagi kesemua tiga arah Cartesian. Dengan menggunakan DOS yang sepadan, kepekatan pembawa pada semua dimensi telah didapati berdasarkan statistik Fermi – Dirac. Tenaga Fermi yang berlandaskan hujung jalur adalah berfungsi kepada suhu yang tidak bergantung pada kepekatan pembawa pada regim tak-merosot. Di regim merosot yang tinggi, tenaga Fermi adalah berfungsi kepada kepekatan pembawa bersesuaian dengan dimensi tersebut tetapi tidak bergantung pada suhu.

**Kata kunci:** Statistik pembawa; kepekatan pembawa; peranti satu-dimensi; pembawa merosot dan tak merosot

### 1.0 INTRODUCTION

As devices are being scaled down in decananometer regime, the physics-based analytical interpretation of carrier statistics in a low-dimensional nanostructure device

<sup>1</sup> School of Engineering & IT, Universiti Malaysia Sabah, 88999, Kota Kinabalu, Sabah

<sup>1–5</sup> Faculty of Electrical Engineering, Universiti Teknologi Malaysia, 81310, Skudai, Johor Bharu

<sup>5</sup> Department of Electrical and Computer Eng., Wilkes University, Wilkes-Barre, PA 18766, USA

\* Corresponding author: Email: [ismail\\_s@ums.edu.my](mailto:ismail_s@ums.edu.my), [ismail\\_saad03@yahoo.com](mailto:ismail_saad03@yahoo.com)

is essentially needed [1–3]. The quantum confinement effect (QCE) and ballistic (B) carrier transport in nano-devices have been heavily investigated and modeled to spur proper understanding of insight of the nano-electronics circuits [4–10]. The numerical analysis of carrier statistics that invoked QCE and B phenomenon of a nanostructure device is elaborated in this paper. The appropriate approximation of Boltzmann and Fermi-Dirac statistics applied to non-degenerate (ND) and degenerate (D) regime for all dimensionality was employed and explained intuitively. The fundamental physics of energy spectrum in the low-dimensional system for quasi 3D, 2D and 1D is presented in Section II. The computation of carrier statistics that leads to proper approximation in all degeneracy level is elucidated in Section III. Section IV provides the results and analysis of carrier statistics in all dimensions of degeneracy and its dependency on carrier concentrations. Major findings of this work are summarized in the concluding Section V.

## 2.0 LOW-DIMENSIONAL ENERGY SPECTRUM

In low-dimensional system as shown in Figure 1, the energy spectrums of the respective system that consists of potential and kinetic energy is given by [6]

$$E_{kd} = E_{co} + \frac{1}{2} \left( \frac{P^2}{m^*} \right) = E_{co} + \frac{\hbar^2}{2m^*} [k_x^2 + k_y^2 + k_z^2] \quad (1)$$

where  $P$  is the momentum,  $k_{x,y,z}$  is the wave vector in three directions and  $d$  is the dimensionality of respective system. For quasi 3 dimensional (Q3D) or bulk semiconductors as depicted in Figure 1(a), all the three Cartesian directions are much larger than the de Broglie wavelength ( $L_{x,y,z} \gg \lambda_D \cong 10$  nm). Therefore the energy spectrum is analog-type in  $x, y$  and  $z$ -direction given by

$$E_{k3} = E_{co} + \frac{\hbar^2}{2m^*} [k_x^2 + k_y^2 + k_z^2] \quad (2)$$

with the wavefunction  $\psi_{k3}(\vec{r})$

$$\begin{aligned} \psi_{k3}(x, y, z) &= \frac{1}{\sqrt{\Omega}} e^{j(\vec{k} \cdot \vec{r})} \\ &= \frac{1}{\sqrt{\Omega}} e^{j(k_x \cdot x + k_y \cdot y + k_z \cdot z)} \end{aligned} \quad (3)$$

This wavefunction describes the propagating waves in all three directions. In Q3D system the traveling wavelength in all 3 directions are traveling waves as shown in the wave function of equation (3).  $k_{x,y,z}$  are the wave vector components with momentum  $\vec{p} = \hbar \vec{k}$ .  $E_{co}$  is the unaltered conduction band edge,  $m^*$  is the carrier effective mass

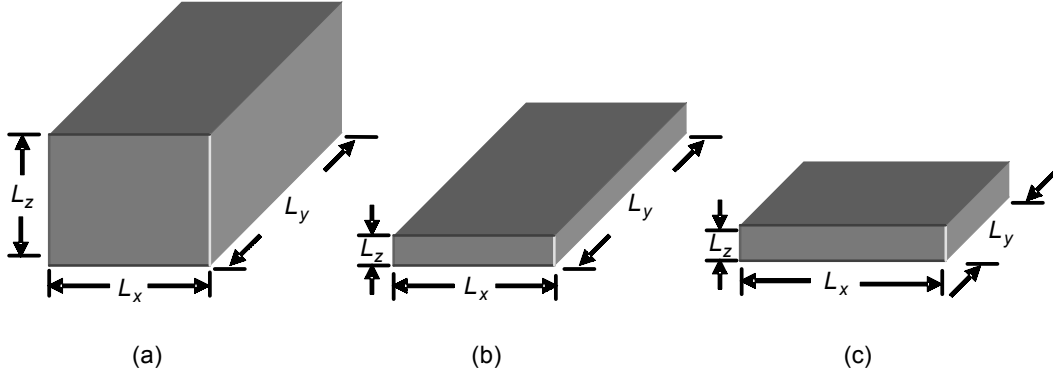


**Figure 1** Low-dimensional system for (a) quasi 3D (b) quasi 2D (c) quasi 1D

assumed isotropic for all three dimensions and  $\Omega = L_x L_y L_z$  is the volume of the samples with  $L_x L_y L_z$  is the length in each of the three Cartesian directions.

Figure 1(b) shows the Q2D of a nano-MOSFET system where the carriers are confined in the  $z$ -direction with  $L_z$  is much less than the de Broglie wavelength ( $D$ ) which is approximately 10 nm. The other two dimensions, the  $x$  and  $y$ -dimensions are still in analogue characteristics with the length  $L_x$  and  $L_y$  are consider larger than de Broglie wavelength. The energy spectrum for Q2D system is given by

$$E_{k2} = E_c + \frac{\hbar^2 k_x^2}{2m_1^*} + \frac{\hbar^2 k_y^2}{2m_2^*} \quad (4)$$

with

$$E_c = E_{c0} + \frac{\hbar^2}{2m_3^*} \left( \frac{\pi}{L_z} \right)^2 \quad (5)$$

and the wave function given by

$$\psi_{k2}(x, y, z) = \sqrt{\frac{2}{\Omega}} e^{j(k_x x + k_y y)} \sin\left(\frac{\pi z}{L_z}\right) \quad (6)$$

Equation (6) shows the wavefunction of a Q2D system where  $L_z$  is the effective length of confinement due to the penetration of the wavefunction in the classical forbidden region. In Q2D system, the wavelength in the  $z$ -direction becomes standing wave due to the quantum confinement (QC) leaving the other two  $x$  and  $y$ -direction retains as traveling waves as shown in the wavefunction expression.  $k_{x,y}$  are the wave vector components with momentum  $\vec{p} = \hbar \vec{k}$  and  $E_c$  is the modified band edge that is lifted by the zero-point quantum energy due to QC effects. The wave-vector is digitized in the  $z$ -direction with the value  $k_z = n\pi/L_z$  with only  $n = 1$  digit being considered in the quantum limit when most electrons occupy the lowest level of band edge. Due to

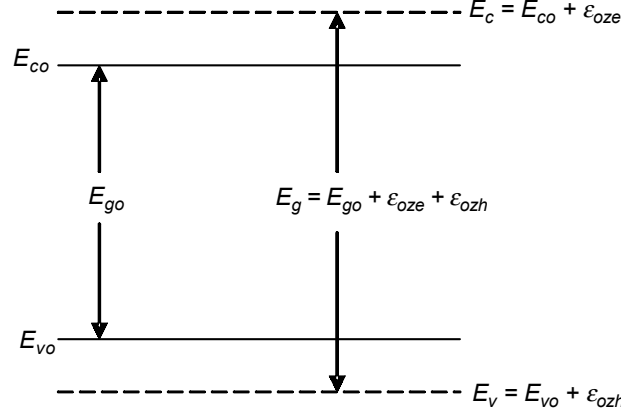


**Figure 2** The modified energy band diagram of Q2D system due to quantum confinement in  $z$ -direction

QC effects in the  $z$ -direction of Q2D system the modified energy band diagram is expected as shown in Figure 2. The energy band gap has been increased by the quantized band edge in  $z$ -dimensions for both conduction and valence band edge with either electron or hole carriers given by

$$\varepsilon_{oze(h)} = \frac{\pi^2 \hbar^2}{2m_{e(h)}^* L_z^2} \quad (7)$$

For Q1D of a nanowire system only one dimension is larger than the de Broglie wavelength. The other two dimensions are quantum confined to the length less than de Broglie wavelength. This system is illustrated in Figure 1(c) in which the length of  $L_z$  and  $L_y$  is confined. Thus, the energy spectrum of Q1D device is only analogue in the  $x$ -direction. The energy spectrum for nanowire with a rectangular cross-section is given by

$$E_{k1} = E_{c1} + \frac{\hbar^2 k_x^2}{2m_1^*} \quad (8)$$

with

$$E_{c1} = E_{co} + \frac{\pi^2 \hbar^2}{2m_1^* L_y^2} + \frac{\pi^2 \hbar^2}{2m_3^* L_z^2} \quad (9)$$

and the wave function given by

$$\psi_{k1}(x, y, z) = \sqrt{\frac{2}{\Omega}} e^{j(k_x \cdot x)} \sin\left(\frac{\pi y}{L_y}\right) \sin\left(\frac{\pi z}{L_z}\right) \quad (10)$$

As depicted in equation (10), for Q1D system the quantum waves are standing wave in  $z$  and  $y$ -direction while in  $x$ -direction it remains as traveling waves.  $E_{c1}$  is the band

edge in the quantum limit of a nanowire that is lifted from bulk conduction band edge  $E_{co}$  by the zero-point energy in the  $y$  and  $z$ -direction.

### 3.0 Low-Dimensional Carrier Statistics

The number of carriers available for conduction determines the electrical properties of the semiconductor devices. This number is found from the density of allowed states and the probability that these states are occupied. The probability that an available state with energy  $E$  is occupied by an electron under thermal equilibrium is given by the Fermi-Dirac probability density function  $\mathfrak{F}(E)$  defined as

$$\mathfrak{F}(E) = \frac{1}{1 + \exp\left(\frac{E - E_F}{k_B T}\right)} \quad (11)$$

where  $E_F$  is the Fermi energy level defined as the energy level at which the probability of finding an electron, for  $T > 0^\circ K$ , is exactly one-half.  $E_F$  is purely mathematical parameter and provides a reference with which other energies can be compared. If  $E = E_F$ ,  $\mathfrak{F}(E) = 1/2$ , this means that the electron is equally likely to have an energy above Fermi level as well as below it. If  $\mathfrak{F}(E) = 1$  at  $T = 0 K$ , this means all energy levels below  $E_F$  are filled and all above it are empty.  $k_B$  is the Boltzmann's constant and  $T$  is semiconductor lattice temperature. If  $E - E_F > k_B T$ , the solution of equation (11) becomes much simpler since we can neglect the '1' and the function  $\mathfrak{F}(E)$  can be approximated by the Boltzmann density function

$$\mathfrak{F}(E) = \exp\left(\frac{E_F - E}{k_B T}\right) \quad (12)$$

The utilization of Boltzmann density function makes subsequent calculation much simpler and normally is justified in semiconductor device theory. However, Fermi-Dirac distribution function is necessary for certain properties of a very highly doped (degenerate) material. Due to recent advanced devices was purportedly to be degenerately doped for the suppression of short channel effects (SCE), the exact solution of Fermi-Dirac distribution function is necessary. The solution is known as Fermi-Dirac Integral of order  $i$  and is given by

$$\mathfrak{F}_i(\eta) = \frac{1}{\Gamma(i+1)} \int_0^\infty \frac{x^i}{e^{(x-\eta)} + 1} dx \quad (13)$$

where

$$\eta = \frac{E_F - E_C}{k_B T} \quad (14)$$

and  $\Gamma$  is the gamma function that can be approximated by

$$\Gamma(i+1) = i\Gamma(i) \quad (15)$$

The number of electrons per unit volume with energies between  $E$  and  $E + dE$  has been established to be  $D(E) \mathfrak{S}(E)dE$ ; therefore the total carrier concentration in a band is obtained simply by integrating the Fermi-Dirac distribution function over energy band that is [5]

$$n = \int_{E_c}^{E_{top}} D(E) \mathfrak{S}(E) dE \quad (16)$$

The carrier concentration ( $n_3$  per unit volume for bulk,  $n_2$  per unit area for 2D, and  $n_1$  per unit length for 1D) as a function of normalized Fermi energy  $\eta_{Fd}$  ( $d = 3, 2, 1$ ) with respect to the band edge is evaluated as [4, 6]

$$n_d = N_{cd} \mathfrak{S}_{\frac{(d-2)}{2}}(\eta_d) \quad (17)$$

Therefore, the electron concentrations for Q3D, Q2D and Q1D system are respectively given as

$$n_3 = N_{c3} \mathfrak{S}_{\frac{1}{2}}(\eta_3) \quad (18)$$

$$n_2 = N_{c2} \mathfrak{S}_0(\eta_2) \quad (19)$$

$$n_1 = N_{c1} \mathfrak{S}_{-\frac{1}{2}}(\eta_1) \quad (20)$$

with the effective density of states respectively defined as

$$N_{c3} = 2 \left( \frac{m^* k_B T}{2\pi \hbar^2} \right)^{\frac{3}{2}} \quad (21)$$

$$N_{c2} = \frac{m^* k_B T}{\pi \hbar^2} \quad (22)$$

$$N_{c1} = \left( \frac{2m^* k_B T}{\pi \hbar^2} \right)^{\frac{1}{2}} \quad (23)$$

The complexity of solving Fermi-Dirac Integral is reduced under the Boltzmann approximation assumption and becomes (for non-degenerately doped devices)

$$\mathfrak{S}_i(\eta) = e^\eta \quad (24)$$

However, as the modern devices are mostly in the degenerately-doped sample, the exact solution of Fermi-Dirac integral is necessary and obtained as [6]

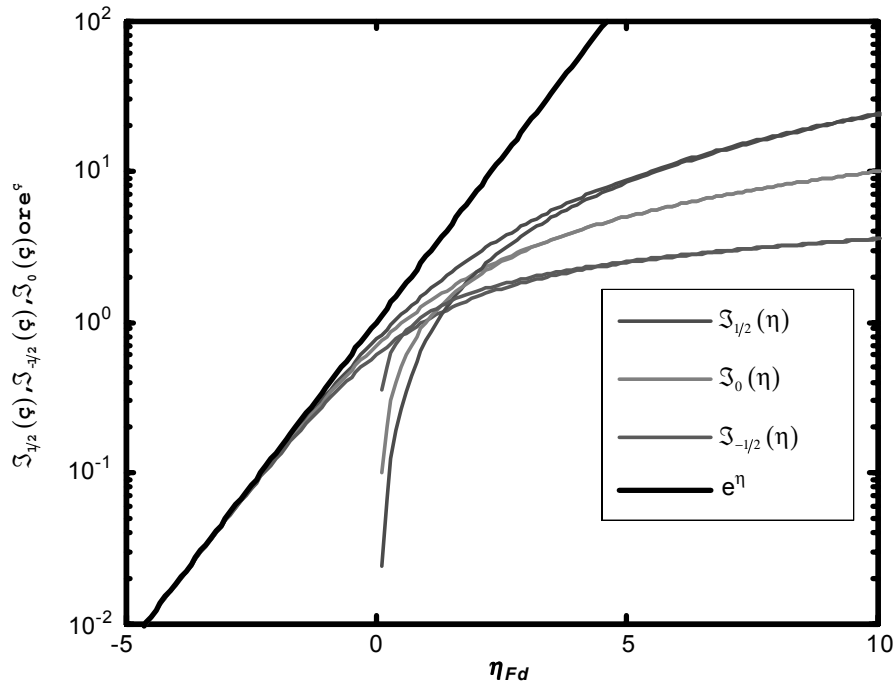
$$\mathfrak{S}_i(\eta) = \frac{1}{\Gamma(i+1)} \frac{\eta^{i+1}}{i+1} \quad (25)$$

#### 4.0 RESULTS AND DISCUSSIONS

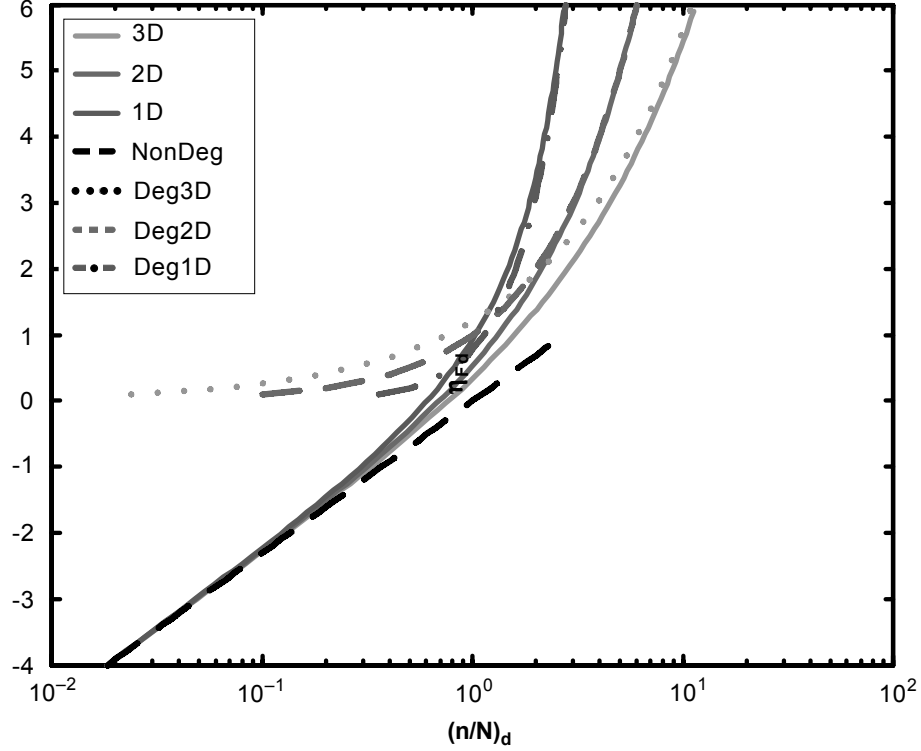
Figure 3 shows the plot of Fermi-Dirac integral of order one-half, zero and minus one-half against fermi energy ( $\eta - \eta_{Fd}$ ) for non-degenerately and degenerately doped samples with  $d = 3, 2, 1$ . In non-degenerately region in which  $\eta_{Fd}$  is small, the Fermi-Dirac integral is well approximated by Equation (24) for all dimensions as indicated by the black color line. Similarly, in degenerately doped devices ( $\eta_{Fd} > 0$ ), the blue, green and red color lines represent the very well estimation of Fermi-Dirac integral of equation (13) to its approximation in 3D (blue), 2D (green) and 1D (red) as can be derived from equations (25) respectively.

Figure 4 shows the normalized Fermi energy  $\eta_{Fd}$  as a function of normalized carrier concentration for  $d = 3, 2, 1$ . As expected in the non-degenerate (ND) regime,  $(E_F - E_c)_d$  as a function of  $(n/N)_d$  is given by

$$(E_F - E_c)_d = k_B T \ln(n/N)_d \quad (26)$$



**Figure 3** The approximation of Fermi-Dirac integral as a function of Fermi energy  $\eta_{Fd}$  for non-degenerately and degenerately doped devices in  $d = 3, 2$  and 1-dimensional system



**Figure 4** The normalized Fermi energy as a function of carrier concentration. Approximation for non-degenerate (ND) regime and degenerate regimes are also shown

$(E_F - E_c)_d$  is a weak (logarithmic) function of carrier concentration, but varies linearly with temperature in the ND regime. However, for strongly degenerate statistics, the Fermi energy is independent of temperature and is a strong function of carrier concentration:

$$(E_F - E_c)_d = \frac{\hbar^2}{m^*} 2\pi \left[ \Gamma\left(\frac{d}{2} + 1\right) n_d / 2 \right]^{2/d} \quad (27)$$

The Fermi energy is proportional to  $n_3^{2/3}$  for bulk (3D) configuration,  $n_2$  for 2D nanostructure, and  $n_1^2$  for 1D nanostructure. The 1D nanowires approach degeneracy at relatively lower values of carrier concentration as compared to 2D and 3D structures. Induced and doped carrier density in most nanoscale devices are now in degenerate regime generating a great interest in degenerate statistics that is extensively used in the following section. Because of simplicity in the expressions for ND statistics, it is not uncommon to base the findings on ND statistics that sometimes leads to erroneous results.



## 5.0 CONCLUSIONS

Based on the low-dimensional energy spectrum that invoked the effect of quantum confinement comparable to the De Broglie wavelength in the respective Cartesian directions of quasi 3D, 2D and 1D, the numerical analysis of nanostructure carrier statistics was successfully done. For non-degenerately (ND) doped samples the Fermi-Dirac (FD) integral is well approximated by Boltzmann statistics for all dimensions. However, in degenerately doped quasi 3D, 2D and 1D device, the FD integral is found to be approximated by order one-half, zero and minus one-half respectively. The Fermi energy is revealed to be a weak (logarithmic) function of carrier concentration, but varies linearly with temperature in the ND regime. However, for strongly degenerate statistics, the Fermi energy is independent of temperature and is a strong function of carrier concentration. The Fermi energy is proportional to  $n_3^{2/3}$  for bulk (3D) configuration,  $n_2$  for 2D nanostructure, and  $n_1^2$  for 1D nanostructure. In addition, the 1D nanowires approach degeneracy at relatively lower values of carrier concentration as compared to 2D and 3D structures.

## ACKNOWLEDGEMENT

The authors would like to acknowledge the financial support from E-Science grant (Vot. No: 79178) of the Ministry of Science, Technology and Innovation (MOSTI). The author is thankful to the Research Management Centre (RMC) of Universiti Teknologi Malaysia (UTM) for providing excellent research environment in which to complete this work.

## REFERENCES

- [1] International Technology Roadmap for Semiconductor (ITRS) - Emerging Research Devices. 2006. 53(5).
- [2] Sizov, D. S. *et al.* 2004. Influence of Carrier Statistics on InGaN/GaN Device Performance. IEEE International Conference of Semiconductor Electronics. ICSE 2004.
- [3] Arora, V. K., 2000. Quantum Engineering of Nanoelectronic Devices: the Role of Quantum Emission in Limiting Drift Velocity and Diffusion Coefficient. *Microelectronics Journal*. Elsevier. 31(11-12): 853–859.
- [4] Arora, V. K. 2008. Ballistic Quantum Transport in Nano Devices and Circuits. 2<sup>nd</sup> IEEE International Nanoelectronics Conference, 2008. INEC 2008. 24-27 March 2008. 573–578.
- [5] Fairus, A. M. T. and V. K. Arora. 2000. Quantum Engineering of Nanoelectronic Devices: the Role of Quantum Confinement on Mobility Degradation. *Microelectronics Journal*. Elsevier. 32: 679–686.
- [6] Ismail Saad, Michael L. P Tan, Ing Hui Hii, Razali Ismail and Vijay K. Arora. 2009. Ballistic Mobility and Saturation Velocity in Low-Dimensional Nanostructures. *Microelectronic Journal*. Elsevier. 40: 540–542.
- [7] Rahman, A., J. Guo, S. Datta and M. Lundstrom. 2003. Theory of Ballistic Nanotransistors. *IEEE Trans. Electron. Devices*. 50: 1853–1864.
- [8] Natori, K. 1994. Ballistic Metal-oxide-semiconductor Field Effect Transistor. *Journal of Applied Physics*. 76(8): 4879–4890.
- [9] Natori, K. 2002. Ballistic MOSFET Reproduces Current-Voltage Characteristics of an Experimental Device. *IEEE Trans. On Electron Devices*. 23(11): 655–657.
- [10] Lundstrom, M. 1997. Elementary Scattering Theory of the Si MOSFET. *IEEE Electron Device Letters*. 18, N.